Radiative heat losses from spherical flames of hydrogen and methane mixtures.

Anthony Roque, Alaa Hamadi, Mahmoud Idir, Andrea Comandini, Nabiha Chaumeix
ICARE-CNRS
1C, avenue de la Recherche Scientifique CS 50060 – 45071, ORLEANS Cedex 2, France.

1 Introduction

Around the globe, there is a rising concern about the effect of CO_2 on the global warming, hydrogen has emerged as an excellent option to phase out fossil fuels from our energy mix. In this sense, the utilization of hydrogen-blended hydrocarbon bio-fuels, or even completely carbon-free fuels like pure hydrogen and ammonia, will be indispensable for emissions reduction from transport and energy production systems.

Understanding the fundamental combustion properties is the basis for the design of combustion devices. The mixing of hydrogen and methane brings a new dimension of complexity that needs to be carefully investigated. Many numerical and experimental studies were performed for on its fundamental combustion properties such us unstretched laminar burning velocity (S_b^0).

S_B^0 has a great importance for turbulent combustion as well as validation and improvement of chemical kinetic schemes [1]. Okafor [2] showed that an increase in hydrogen concentration in the binary fuel led to an increase in the S_b^0 and the Markstein length (L_b) changed non-monotonically. The hydrogen addition with methane mixture (binary fuel) in different engine systems (such as port fuel injection and direct injection engines) resulted in higher thermal efficiency, reduction of combustion duration and ignition delay [3]. From the different methods to determine laminar flame speeds, the spherically expanding flame configuration (SEF) presents many advantages especially in terms of initial pressure, temperature, and gas composition. The stretched flame speed (S_b) and stretch rate are calculated from the temporal flame front history.

Chen [4] identified that the discrepancies in the laminar flame speeds and Markstein lengths measured by different researchers for the same fuel and reported in the literature. The author pointed as source of those variation to the non-appropriate correction taking account radiation and compression when SEF method is used. Flame radiation intensity and spectral distribution are strongly dependent on flame dimensions and shape as well as mixture (fresh and burned gases) composition, and local pressure and temperature [5].

The complexity involved in identify the right species with the right transport phenomena in the numerical models to correct radiation loss such us optically thin model (OTM) or Statistical narrow band model (SNB) was pointed by different authors [4, 6].

Correspondence to: anthony.roque-ccacya@cnrs-orleans.fr

The goal of this study is to assess the best procedure to analyze the radiative heat losses by a spherical flame of mixtures a mixture of CH_4 and H_2. The signal was captured using Fast Absolute Infra-Red Sensor (FAIRS) already tested with prelaminar results presented by Idir et al. [5]. The quantification of the percentage of radiation lost by the expanding flames is our target.

To the best of our knowledge, there is yet no investigation reported on heat losses experimentally determined.

2 Experimental Setup

The experiments using the SEF method were performed in a spherical constant volume vessel of 56 liters. Experimental details about the procedure and the method can be found in [7]. The Fast Absolute Infra-Red Sensor (FAIRS) was located in one side looking to the center of the vessel, where ends of two tungsten electrodes generate the spark ignition, see Fig. 1a. The flame propagation is recorded by a fast camera PHANTOM v1610, the signal of the internal pressure and infrared emission of the flame is collected by FAIRS sensor as observed in Fig. 1c. The fundamental principles on the radiation sensor can be found in [5].

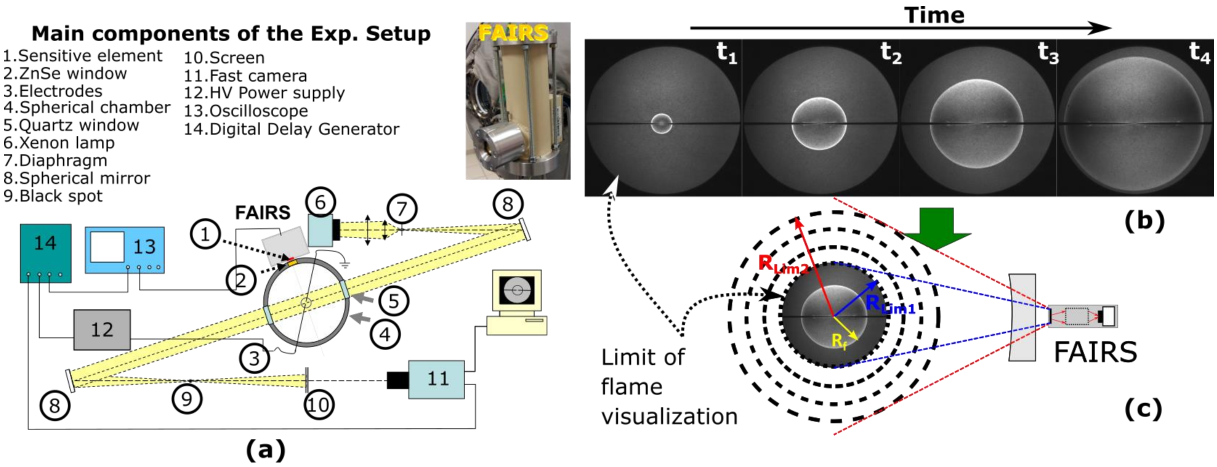

Figure 1: (a) main components of the experimental setup; (b) spherical flame propagation; (c) capture of heat radiation from the combustion process.

Due to the small-time scales used (around 40 ms), the noise from the signals from the infrared and pressure was filtered using mobile smoothing, Savitzky-Golay and fast Fourier transform filters. After that, a fitting curve was set for the both signals as observed in Fig. 2.

A radius extrapolation was done for an adjustment of a polynomial fit which was compared with the integrated solution for a quasi-steady nonlinear model.

$$\left(\frac{S_b}{S_b^0}\right)^2 ln\left(\frac{S_b}{S_b^0}\right)^2 = -\frac{L_b \kappa}{S_b^0}$$

$$R_f + 2L_b ln\left(R_f\right) - 4\frac{{L_b}^2}{R_f}\frac{8}{3}\frac{{L_b}^3}{{R_f}^2} = tS_b^0 + C$$

Where R_f is the radius of the flame, κ is the Stretch, t is the time and C is a constant of integration of the velocity equation of the non-linear model [8]. Most of the graphs use the radius as abscissa axis which is refer to the polynomial fitting for the radius extracted from the flame propagation images.

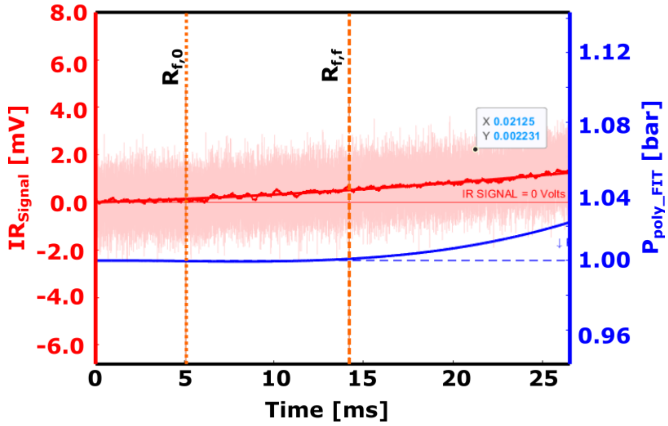

Figure 2: fitting curves of the infrared signal (solid red line) captured with FAIRS sensor and the fitting curve for pressure (solid blue line).

3 Results: Dimensional Transformation of signals

The total flux ($\dot{Q}_{IR,loss}$) can be estimated using the calibration factor deduced to spherical flames, the attenuation induced by the ZnSe window was taking in count [5].

$$\dot{Q}_{IR,loss}[W] = 555000 \times Q_{IR}[V]$$

Where Q_{IR} is the measured IR signal in Volts.

The theorical estimation of the energy released along the flame expansion can be performed. This allows to estimating the lost radiative energy proportion. As indicated in the previous section, the flame radius (R_f) is extrapolated for earlier and later times. Therefore, the flame volume can be determined as equivalent to the volume of mixture burned until this moment ($V_{mix}(t)$). The initial flame propagation stages can be considered as an isentropic expansion, which allows calculate the fresh mixture temperature (T_{mix}) if the instantaneous pressure is known ($P_{mixture}(t)$). With the values of V_{mix}, $P_{mixture}$, T_{mix} and using the ideal gas law equation, the total number of moles of the mixture that will be burned can be estimated at each time. However, there are some final remarks before to multiply the consumed moles by the heat of combustion ($\Delta H_{Rx,fuel}$) that should be taken in account, as observed in the next equation.

$$\frac{dQ}{dt} = \Delta H_{Rx,fuel}\left[\frac{J}{mol\_fuel}\right] \times N_{Total\_fuel}(t) = \Delta H_{Rx,fuel}\left[\frac{J}{mol\_fuel}\right] \times [N_{H2}(t) + N_{CH4}(t)]$$

The determination of $\Delta H_{Rx,fuel}$ depends on the initial temperature and the quantity of air available because under rich condition the water-gas reaction shift reaction should be considered ($CO_2 + H_2 \leftrightarrow CO + H_2O$). $\Delta H_{Rx,fuel}$ was determined using the molar fractions of main species using COSILAB.

The above described procedure was applied to six consecutive experiments of a mixture of 10% H_2+ 90% CH_4. The initial conditions for those experiments were $ER = 1.0$;$T_0 = 308K$ at $P_0 = 2bar$. Fig. 3 shows pictures of the flames at almost the same time of acquisition (around 0.01s). Two of the flames were very smooth (M217 and M219) and the others presented small deformations due to the ignition.

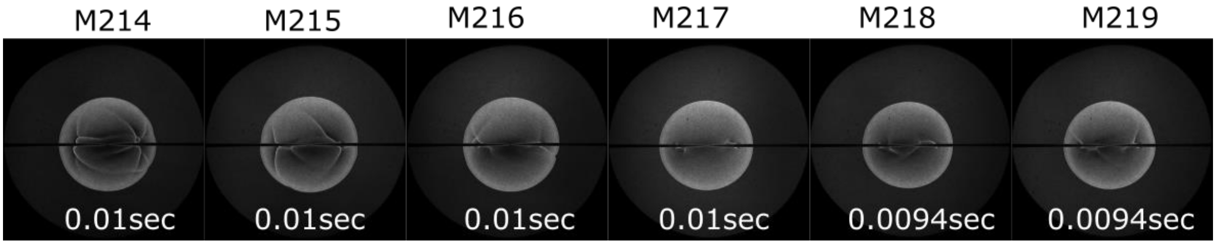

Figure 3: Picture of the flames considered in the repeatability study. Initial conditions 10% H_2 + 90% CH_4; $ER = 1.0$;$T_0 = 308K$; $P_0 = 2bar$.

Fig. 4 presents the main results of the analysis proposed in this paper. Fig 4a shows the pressure profiles for the six experiments. The values are obtained after the application of Savitzky-Golay filter as mentioned in the previous section. In order to remove any noise from the pressure signal a polynomial fit was used to get the profiles presented in Fig 4b, this will be useful after to perform the dQ/dt calculations. A small discrepancy in the pressure values of 0.02bar for M219 is identified. Fig. 4c confirms that the discrepancy in M219 didn't play a big impact on the calculation of dQ/dt. However, this perturbation could have had influence the variation in the radiation signal presented at Fig. 4d. This figure shows the value of the simulated non-stretch flame speed estimated by GRI3.0 and Curran2008 mechanism, the values of the experimental values appears for each experiment next to each radiative curve. The values between experimental values and calculation are not so far. A zoom applied to the bottom part of the curves allows to observe small differences between the different curves since the start, around a $R_f = 10mm$. Finally, observing the Fig 4e allows us to have an initial approximation of the percentage of energy lost by radiation. However, some simplifications were done in the procedure to calculate the heat release such as not consider the variation in the densities due to the small increase of the pressure in the region of analysis. This could have a considerable effect at on the beginning stage of the combustion process which will be corrected later. In addition, it is important to observe the different increasing trend for M217 experiment, this could be associated to the fitting method used. Another behavior observed was the high sensibility of FAIRS sensor when the composition of the mixture changes, this behavior is not presented. The last can be associated to change in level of the reached adiabatic temperature favorized by the higher absoprtion properties of CO_2 and H_2O, due to difference in radiative properties, , Rivière [9].

4 Summary and conclusions

Heat losses of a spherical flame propagation were measured using an infrared detector developed and tested in similar configuration. Repetitive measurements showed that some level of variation can be expected of the infrared fitting signal even for experiments preformed consecutively. A method to quantify the radiative heat losses from was proposed to get an initial approximation of the fraction lost by radiation. Despite the value got around 1%, futures improvements will be done in the methodology to improve and validate this initial estimation.

5 Acknowledgements

The authors acknowledge the financial support of la Fédération EPEE (Énergétique, propulsion, espace, environnement). A. Roque is supported by the French National Science Foundation, ANR, Grant ANR-PHYSSA, Grant agreement no. ANR-20-CE05-0014-01

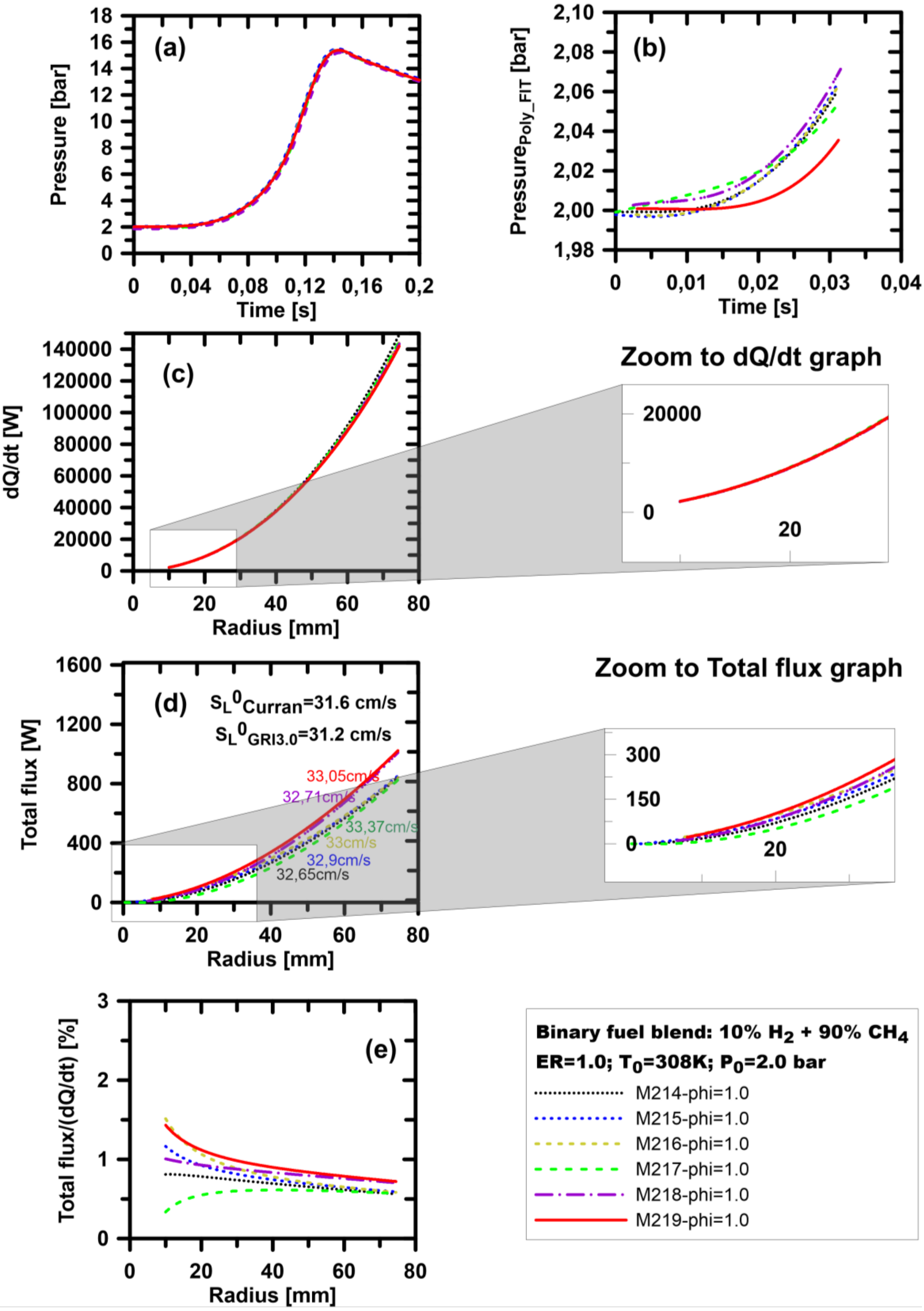

Figure 4: Main result for the calculation of the fraction of radiative heat loss for a flame at 10% H_2+ 90% CH_4; $ER = 1.0$;$T_0 = 308K$; $P_0 = 2bar$: (a) Experimental filtered pressure; (b) fitted pressure; (c) instantaneous heat release, dQ/dt; (d) Total flux and (e) percentage of heat loss in function of radius.

References

[1] J. Beeckmann, R. Hesse, J. Schaback, H. Pitsch, E. Varea, and N. Chaumeix, "Flame propagation speed and Markstein length of spherically expanding flames: Assessment of extrapolation and measurement techniques," *Proceedings of the Combustion Institute*, vol. 37, no. 2, pp. 1521–1528, 2019, doi: 10.1016/j.proci.2018.08.047.

[2] E. C. Okafor, A. Hayakawa, Y. Nagano, and T. Kitagawa, "Effects of hydrogen concentration on premixed laminar flames of hydrogen-methane-air," *Int J Hydrogen Energy*, vol. 39, no. 5, pp. 2409–2417, Feb. 2014, doi: 10.1016/j.ijhydene.2013.11.128.

[3] F. Catapano, S. di Iorio, P. Sementa, and B. M. Vaglieco, "Analysis of energy efficiency of methane and hydrogen-methane blends in a PFI/DI SI research engine," *Energy*, vol. 117, pp. 378–387, Dec. 2016, doi: 10.1016/j.energy.2016.06.043.

[4] Z. Chen, "Effects of radiation and compression on propagating spherical flames of methane/air mixtures near the lean flammability limit," *Combust Flame*, vol. 157, no. 12, pp. 2267–2276, Dec. 2010, doi: 10.1016/j.combustflame.2010.07.010.

[5] M. Idir, A. M. Rayaleh, D. de Sousa Meneses, N. Semmar, and N. Chaumeix, "Absolute and real time experimental radiative loss measurements of spherical expanding free flames: FAIRS (Fast Absolute InfraRed Sensor) - An innovative technique," *Review of Scientific Instruments*, vol. 93, no. 9, Sep. 2022, doi: 10.1063/5.0101519.

[6] S. Zheng *et al.*, "Effects of radiation reabsorption on the laminar flame speed and NO emission during aviation kerosene combustion at elevated pressures," *Fuel*, vol. 324, Sep. 2022, doi: 10.1016/j.fuel.2022.124545.

[7] A. Comandini, G. Pengloan, S. Abid, and N. Chaumeix, "Experimental and modeling study of styrene oxidation in spherical reactor and shock tube," *Combust Flame*, vol. 173, pp. 425–440, Nov. 2016, doi: 10.1016/j.combustflame.2016.08.026.

[8] M. J. Hegetschweiler *et al.*, "Data reduction considerations for spherical R-32(CH2F2)-air flame experiments," *Combust Flame*, vol. 237, Mar. 2022, doi: 10.1016/j.combustflame.2021.111806.

[9] Rivière P; Soufiani A. Updated band model parameters for H2O, CO2, CH4 and CO radiation at high temperature. International Journal of Heat and Mass Transfer 55 (2012) 3349–3358.